CHEMISTRY
A EUROPEAN JOURNAL

DOI: 10.1002/chem.200600672

Mimicking Enzymes: Cooperation between Organic Functional Groups and Metal Ions in the Cleavage of Phosphate Diesters

Monica Livieri,[a] Fabrizio Mancin,*[a] Giacomo Saielli,[b] Jik Chin,[c] and Umberto Tonellato[a, b]

Abstract: A series of ligands derived from the bis-2-pyridinylmethylamine structure, which bear either additional hydroxyl or aromatic amino groups, were prepared and their Zn^{II} complexes were studied as catalysts for the cleavage of bis-*p*-nitrophenyl phosphate (BNP) and 2-hydroxypropyl-*p*-nitrophenyl phosphate (HPNP) diesters. A comparative kinetic study indicated that the insertion of organic groups, capable of acting as nucleophiles or as hydrogen-bond donors, substantially increases the hydrolytic activity of the metal complex. Dissection of the effects of the individual groups revealed that the increase in reactivity can reach up to three orders of magnitude. The improved efficiency of the systems studied, combined with the benefits resulting from the low pK_a value of the active nucleophile, result in an acceleration of the BNP cleavage at pH 7 of six orders of magnitude. The pH-dependent reactivity profiles follow a bell-shaped curve and the maximum reactivity is observed at pH 9. The mechanism of the reactions and the structure of the complexes were investigated in detail by means of kinetic analysis, NMR spectroscopy experiments, and theoretical calculations. The reactivity of the complexes that cleave HPNP closely resembles the reactivity observed for BNP, but the accelerations achieved are lower as a result of different reaction mechanisms.

Keywords: artificial nucleases · catalysis · hydrogen bonds · hydrolysis · phosphate diesters

Introduction

Despite the exceptional resistance of phosphate diesters towards hydrolytic scission,[1] the manipulation of nucleic acids in living organisms continuously requires the cleavage of phosphodiester bonds. In nature the problem was solved by the evolution of nucleases, which are enzymes that accelerate the hydrolysis of nucleic acids up to 10^{16}-fold, thus making possible the DNA and RNA manipulations essential to life.[1] Many nucleases are metalloenzymes that take advantage of the Lewis acidity of the metal ions, in particular Zn^{II}, Mg^{II}, and Fe^{III}, to increase the reactivity of both the substrate and the reacting species.[2] In fact, such metal centers can play several catalytic roles, for example, Lewis acid activation of the substrate, transition-state stabilization, nucleophile generation, and leaving-group stabilization.[1,3] The high reactivity of nucleases is also a consequence of the presence of many organic groups, belonging to the amino acid residue side chains, in their active sites. These organic residues can provide reactive nucleophiles and show very effective catalytic behavior through hydrogen-bonding and electrostatic interactions.[2]

Several examples of synthetic systems, mainly based on metal complexes, capable of accelerating the hydrolysis of nucleic acids or model phosphate esters have been reported recently.[4] The interest in such systems is stimulated by the possibility of providing useful alternatives to the restriction enzymes currently used as laboratory tools in biotechnology and molecular biology.[4f] More distant but still an attractive target is the potential for such systems to act as anticancer, antiviral, and antibiotic drugs.[4d] Unfortunately, the activity of artificial systems is still much lower than the corresponding enzymes, despite the promising results that have been achieved recently by using dinuclear Ce^{IV} or Fe^{III} catalysts.[4a]

[a] Dr. M. Livieri, Dr. F. Mancin, Prof. U. Tonellato
Dipartimento di Scienze Chimiche, Università di Padova
via Marzolo 1, 35131 Padova (Italy)
Fax: (+39) 049-827-5239
E-mail: fabrizio.mancin@unipd.it

[b] Dr. G. Saielli, Prof. U. Tonellato
Istituto CNR per la Tecnologia delle Membrane, via Marzolo 1
35131 Padova (Italy)

[c] Prof. J. Chin
Department of Chemistry, University of Toronto
80 St. George Street, M5S 3H6 Toronto (Canada)

Supporting information for this article is available on the WWW under http://www.chemeurj.org/ or from the author.

In the search for more reactive agents, one possible solution is to add strategically located organic functional groups to the ligand structure that are capable of enhancing the catalyst activity.[5] Examples of such systems are few, but the results obtained to date are encouraging. Early work by Breslow and co-workers showed that the insertion of thiophenol or imidazole subunits into Zn^{II} complexes of tetradentate macrocyclic ligands increases the rate of cleavage of the RNA model compound 2-hydroxypropyl-*p*-nitrophenyl phosphate (HPNP) by one order of magnitude, probably through general base catalysis.[6] Subsequently, the groups of Chin and Kimura demonstrated that adding a hydroxyl group to the ligand can provide a more powerful nucleophile than the water molecule bound to the metal ion.[7] Krämer and Kövári demonstrated that introducing a dimethylammonium group in a specific orientation in a bipyridine-based Cu^{II} complex increases the hydrolysis activity of the complex towards the DNA model compound bis-*p*-nitrophenyl phosphate (BNP) by three orders of magnitude, as a result of hydrogen-bond and charge stabilization of the reaction transition state.[8] In a similar system, based on the Zn^{II} complex of a terpyridine ligand bearing two guanidinium groups, Anslyn and co-workers observed a rate acceleration for the hydrolysis of RNA dinucleotide ApA at pH 7.4 at 37 °C of three orders of magnitude with respect to the complex without guanidinium groups.[9] Turning their attention to hydrogen bonds, Chin and co-workers showed that by using the hydrogen-bonding ability of two amino groups in the Cu^{II} complex of 2,8-diaminophenanthroline a tenfold increase in the catalytic ability of the system towards BNP cleavage is produced.[10] Recently, Mareque-Rivas, Williams, and co-workers found that the presence of three hydrogen-bond-donating amino groups in the Zn^{II} complex of tris(2-amino-6-pyridinylmethyl)amine increases the rate of HPNP transesterification by almost three orders of magnitude.[11,12]

In contrast to the structural versatility of enzymes, all the examples previously given integrate a single type of organic functionality into the metal complex. In a recent communication, we described a Zn^{II} complex that featured both hydrogen-bond-donating amines and a nucleophilic hydroxyl group.[13] The results indicated that the cooperation of different functional organic groups with the metal center leads to an increase in BNP cleavage in a similar manner to enzyme catalysis. In this paper, we report a full account of the reactivity of these previously reported and related complexes.

Results

Zn^{II} complexes characterization: Synthesis of ligands **1**–**5** is described in the Supporting Information. The ligands are soluble in water (up to 1.5 mM at room temperature) and form 1:1 complexes with Zn^{II} ions, as determined by means of potentiometric titrations. These titrations also allowed the evaluation of the pK_a values of the amino groups (pK^n), the formation constant of the Zn^{II} complexes (log K_f), and the pK_a values of the species bound to the metal ion (pK_a^n) (Table 1).

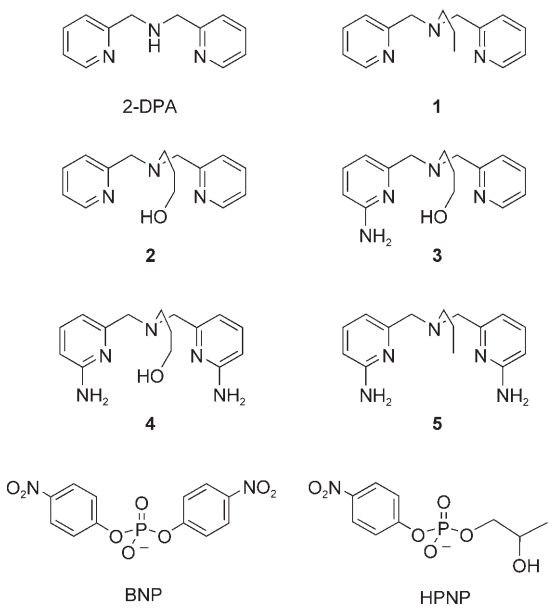

Table 1. Deprotonation constants (pK^n) for the protonated ligand, Zn^{II}-complex-formation constants (log K_f), and deprotonation constants for metal-bound species (pK_a^n) of ligands **1**–**5** determined by means of potentiometric titrations.[a]

Ligand	H_3L^{3+} pK^1	pK^2	pK^3	$[Zn^{II}(L)]^{2+}$ log K_f	pK_a^1	pK_a^2
2-DPA[b]	7.30	2.60	<2	7.57	–	–
1[c]	7.04	2.59	<2	7.82	8.55	10.59
2	6.57	3.06	<2	7.64	8.57	10.70
3	7.32	4.16	<2	7.58	8.51	10.54
4[c]	7.72	5.33	1.95	6.68	7.94	9.96
5[c]	8.14	5.04	2.01	6.92	8.01	10.18

[a] 0.1 M NaCl, 25 °C; estimated errors in the values of these thermodynamic constants are within 5 %. [b] Bis(6-pyridinylmethyl)amine taken as reference ligand, see ref. [14]. [c] See ref. [13].

Inspection of the data reveals that insertion of the 2-amino group into the complex results in an increase in the deprotonation constants for the protonated ligands (pK^n), which is to be expected on the basis of the electron-donating ability of the amino groups. However, it is rather surprising that there is a decrease in formation constants for the Zn^{II} complexes for ligands **4** and **5**, which bear two 2-amino groups, because a greater basicity should correspond to an increased metal-ion affinity for the binding atoms. Overall, the K_f values are high enough to ensure that in each case more than 95 % of the complex is formed above pH 7 (see distribution diagrams in the Supporting Information).

In all the complexes, two metal-bound species that could be deprotonated were detected (pK_a^n), which can be identified as metal-coordinated water molecules and possibly, for the Zn^{II} complexes of **2**, **3**, and **4**, as the ligand hydroxyl group. Again, the presence of the two 2-amino groups on

the pyridine moieties affects the acidity of such species by inducing a 0.5–0.6 decrease in pK_a values. On the other hand, the effect of a single amino group on the pK_a value, as in Zn^{II}–**3**, is apparently negligible.

^{1}H NMR spectra obtained for **4** and Zn^{II}–**4** dissolved in D_2O (Figure 1, also see the Supporting Information) confirm

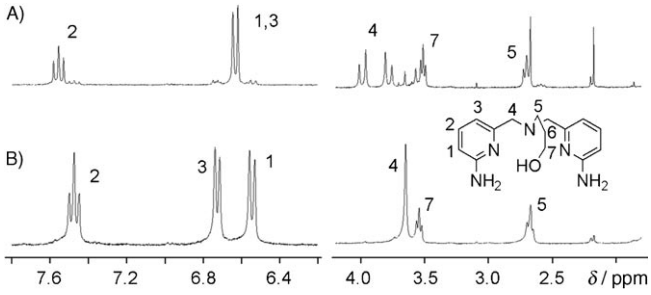

Figure 1. ^{1}H NMR spectra of A) Zn^{II}–**4** and B) **4** at 0.8 mM in D_2O at 28 °C.

the formation of a 1:1 complex, but the chemical shift changes of the signals of the hydroxypropyl-arm methylene groups are very small and did not allow us to determine with certainty whether the hydroxyl group is bound to the Zn^{II} ion or not. To obtain more insight into this point ^{1}H NMR spectra were recorded at pD 7–11. As the pD increases, the signals of the pyridine rings are substantially unaffected, whereas the signals for the hydroxypropyl arm undergo a $\delta = 0.1$ ppm downfield shift that spans the entire pD range explored. The shape of the chemical-shift change versus pD profile (Figure 2) indicates that such variations can be attributed to the deprotonation of the two metal-bound species.

Unfortunately, it was not possible to obtain single crystals of the complexes of ligands **1**–**5** that were suitable for X-ray structure determinations. However, important insight into the structures and properties of the Zn^{II} complexes of **2** and **4** were obtained by means of theoretical studies. Recently, this approach was successfully applied to the analysis of the acidity and nucleophilicity of Zn^{II}-bound species.[15] The complex structures used in the calculations were based on two main assumptions: 1) the ligand alkoxy group (when present) was coordinated to the metal ion on the basis of the results of NMR spectroscopy experiments, and 2) a fifth coordination site on the metal ion was saturated with a water molecule in accordance with potentiometric titrations. The structures of the two possible mono-deprotonated complexes, namely, the Zn^{II} alkoxide and Zn^{II} hydroxide species, were optimized at the density functional theory (DFT) level (see the Experimental Section) by following three different protocols. The calculations were performed in the gas phase, in the gas phase with the addition of one explicit water molecule, and by using the polarizable continuum model (PCM) of solvation (Table 2).

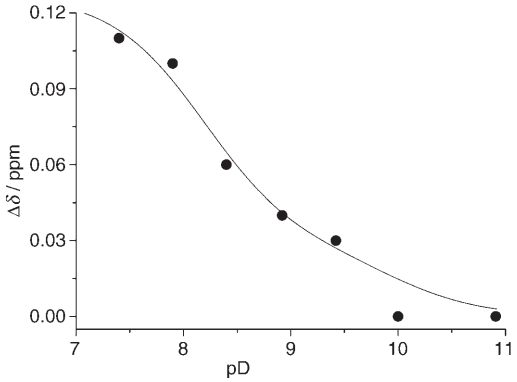

Figure 2. Chemical shifts variations of the signal for proton H5 in Zn^{II}–**4** as a function of the solution pD. The line corresponds to the fit of the data with a model involving two deprotonation equilibria (see the Experimental Section). Conditions: $[Zn^{II}$–**4**$] = 3$ mM, 28 °C.

Literature results for closely related complexes indicate that the energy difference between the two mono-deprotonated species, optimized in the gas phase or by using a solvent model, are similar.[15b] Our computational analysis indicates that the energy difference between the alkoxide and the hydroxide complexes is greater when the solvent model is introduced into the calculations (Table 2). On the other hand, the energy difference between the two species optimized in the gas phase with the addition of a single explicit solvent molecule was similar to that obtained by using the PCM solvent model (Table 2).[16] For this reason, we performed the following calculations by using the former protocol.

Inspection of the optimized structures (Figure 3) reveals that the donor atoms around the Zn^{II} ion are arranged in a distorted trigonal-bipyramid geometry, in which the equatorial positions are occupied by the two pyridine nitrogen atoms and the hydroxyl group, whereas the apical positions are occupied by the tertiary amino group and the water molecule. A whole network of hydrogen bonds between the

Table 2. Comparison of electronic energies (in hartree) for different mono-deprotonated **2** and Zn^{II}–**4** complexes by using different optimization protocols.

	Gas phase	Solvent model[a]	Gas phase (one explicit water molecule)
$[Zn^{II}$(**4**-OH)OH$]^+$	−2788.603968	−2788.688891	−2865.089990
$[Zn^{II}$(**4**-O)$H_2O]^+$	−2788.601416	−2788.680174	−2865.078558,[b] −2865.080899[c]
ΔE [kcal mol^{-1}][d]	−1.6	−6.4	−7.2,[b] −5.8[c]
$[Zn^{II}$(**2**-OH)OH$]^+$	–	–	−2754.299796
$[Zn^{II}$(**2**-O)$H_2O]^+$	–	–	−2754.299051
ΔE [kcal mol^{-1}][d]	–	–	−0.2

[a] PCM continuous solvent model. [b] Structure shown in Figure 3B. [c] Structure shown in Figure 3C. [d] $\Delta E = E_{hydroxide} - E_{alkoxide}$.

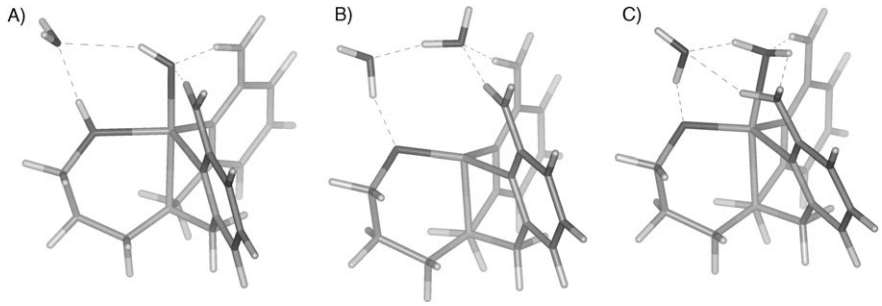

Figure 3. B3LYP/6-311++G(d,p)-optimized structures of Zn^{II}–**4** hydroxide (A) and alkoxide (B, C) complexes (hydrogen bonds are represented by the dashed lines).

metal-bound species, the solvent water molecule, and when present, the ligand 2-amino groups was detected. For the Zn^{II} complexes of **2**, the energies of the two deprotonated species are very similar. A comparable result was reported by Tang and co-workers for a related Zn^{II} complex with bis-2-pyridinylmethyl-2-ethanolamine.[15b] This result implies that the first deprotonation of the metal complex can occur at the two sites (either at the metal-bound water molecule or at the hydroxyl group) with similar probability. On the other hand, for the Zn^{II}–**4** complexes, the energy of the hydroxide species is about 5–6 kcal mol^{-1} lower than that of the alkoxide (Table 2). As expected, the presence of two intracomplex hydrogen bonds between the pyridine 2-amino donors is responsible for the extra stabilization of this species.

The two minimum-energy structures for the alkoxide species of complex Zn^{II}–**4** differ by only 1.4 kcal mol^{-1} (Figure 3B and C) and were obtained from slightly different initial geometries. In the first structure (Figure 3B), the water molecule receives two hydrogen bonds from the ligand 2-amino groups but is held too far away from the metal ion to be effectively coordinated to it. In the second one (Figure 3C), the water molecule is bound to the Zn^{II} ion but only receives one hydrogen bond.[17]

Reactivity toward BNP: Incubation of the Zn^{II} complexes of **2**–**5** with BNP in water at 25 °C results in substrate cleavage; no detectable reaction occurs with Zn^{II}–**1** under the same experimental conditions. The kinetic studies were performed by monitoring the increase of the *p*-nitrophenoxide absorbance at $\lambda = 400$ nm by means of the initial rates method. In each case, the BNP cleavage rate is first-order in both the metal complex and substrate over the concentration range explored (Zn^{II} complexes 1×10^{-4}–1×10^{-3} M; BNP 5×10^{-4}–5×10^{-3} M). Apparent second-order rate constants were obtained at each pH value by the linear fit of the pseudo-first-order rate constants versus complex concentration data. The pH dependence of the apparent second-order rate constants are reported in Figure 4.

The pH profiles show a bell-shaped pattern with a maximum reactivity at around pH 9–9.5.[13] This behavior is diagnostic of the deprotonation of two acidic functions in the metal complex, in which the first deprotonation event leads to an increase in reactivity and the second event leads to the opposite effect. Fitting the pH profiles to a kinetic model involving two deprotonation equilibria (see the Experimental Section) allowed the determination of pK_a values for the reacting species and the second-order rate constants for the reactive mono-deprotonated metal complex (see Table 3, which also shows the kinetic data for HPNP). The resulting kinetic pK_a values are in good agreement with those of the metal-bound acidic species obtained from potentiometric titrations. Comparison of the second-order rate constants in Table 3 reveals the reactivity order of the complexes: Zn^{II}–**4** > Zn^{II}–**5** ≈ Zn^{II}–**3** > Zn^{II}–**2**. The reactivity of complex Zn^{II}–**4** is particularly remarkable: the rate of spontaneous hydrolysis of BNP at pH 7.0 and 25 °C can be estimated to be 1.6×10^{-11} s^{-1} on the basis of the activation parameters determined at high temperatures,[18] while BNP is cleaved by Zn^{II}–**4** (1 mM) at a

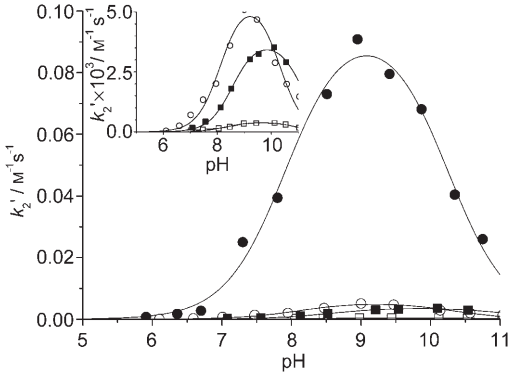

Figure 4. pH dependence of the apparent second-order rate constants (k_2') for the reaction between BNP and Zn^{II} complexes of ligands **2** (□), **3** (■),**4** (●), **5** (○) at 25 °C ([ligand] = [Zn^{II}] = 0.5–1.0 × 10^{-3} M, [BNP] = 2 × 10^{-4} M, [buffer] = 5.0×10^{-2} M). Inset: magnification of the profiles for the complexes of ligands **2**, **3**, and **5**.

Table 3. Kinetic acid dissociation constants for the coordinated species (pK_a^n) and second-order rate constants (k_2) for BNP and HPNP cleavage by using Zn^{II} complexes of ligands **1**–**5** in water at 25 °C.[a]

	BNP			HPNP		
Ligand	pK_a^1	pK_a^2	k_2 [M^{-1}s^{-1}]	pK_a^1	pK_a^2	k_2 [M^{-1}s^{-1}]
1	–[b]	–[b]	–[b]	9.1	10.9	3.9×10^{-2}
2	8.3[d]	10.9[d]	4.2×10^{-4}[d]	8.8	10.9	2.1×10^{-2}
3	8.6	11.0	3.8×10^{-3}	–[c]	–[c]	–[c]
4	7.9[d]	10.2[d]	9.7×10^{-2}[d]	7.2	10.4	2.8×10^{-1}
5	8.1[d]	10.3[d]	5.6×10^{-3}[d]	7.7	10.5	2.8×10^{-1}

[a] [Buffer] = 5.0×10^{-2} M, estimated errors in the values of these kinetic constants are within 10%. [b] No reactivity observed. [c] Not determined. [d] See ref. [13].

rate of $(1.1\pm0.1)\times10^{-5}\,s^{-1}$, with an acceleration close to six orders of magnitude.

To investigate the nature of the reaction products, and in particular, to identify the active nucleophilic species for the BNP cleavage promoted by ligands **2**, **4**, and **5**, a ^{31}P NMR spectroscopy investigation of the reactions was performed (see the Supporting Information). During early stages of the reaction, the cleavage of BNP leads to different products, which depend on the presence of the hydroxyl group in the ligand.[13] In the case of Zn^{II}–**5** (Figure S7 in the Supporting Information), only *p*-nitrophenyl phosphate monoester (MNP) was detected in the ^{31}P NMR spectrum as a reaction product (together with *p*-nitrophenoxide detected in the ^{1}H NMR spectrum of the reaction mixture), as expected from a clean hydrolytic cleavage. For complexes of **2** and **4** (Figures S8 and S9, respectively, in the Supporting Information), the ^{31}P NMR spectra of the reaction mixture show the appearance of a different signal, a triplet at about $\delta=-9.5$ ppm, which can be attributed to the O-phosphorylated ligand that results from a transesterification reaction.[19] The presence of Zn^{II}–**4** and BNP in equimolar amounts in the reaction mixture results in the complete conversion of BNP into the O-phosphorylated ligand. All of these results indicate that the nucleophiles involved in the cleavage reaction are different depending on the ligand structure; the nucleophile is an OH group for **2** and **4** and a water molecule for **5**. Prolonged experiments (Figures S8 and S9) showed that neither the *p*-nitrophenyl phosphate produced in the reaction with the Zn^{II}–**5** complex, nor the phosphorylated ligand formed by **4** undergo further cleavage. However, if an excess of BNP is incubated with the Zn^{II}–**4** complex then the formation of two products is observed (Figure S10 in the Supporting Information). First, the relatively fast formation of the O-phosphorylated ligand is observed, and subsequently, *p*-nitrophenyl phosphate slowly appears, while the amount of O-phosphorylated ligand present in the reaction mixture remains constant.

In addition to the NMR spectroscopy experiments, spectrophotometric investigations performed in the presence of excess substrate revealed a "burst" kinetic profile (Figure 5A). The profile shows an initial fast absorbance increase that corresponds to the release of one equivalent of *p*-nitrophenoxide (with respect to the metal complex) followed by a slower increase of absorbance. Alternatively, kinetic runs performed in the presence of excess Zn^{II}–**4** show saturation profiles (Figure 5B) with an absorbance increase that corresponds to the release of two equivalents of *p*-nitrophenoxide.

Reactivity toward HPNP: Incubation of HPNP, with all the Zn^{II} complexes of ligands **1**, **2**, **4**, and **5** results in substrate cleavage. The mode of reaction is different from that of BNP. According to NMR spectroscopy investigations, the only reaction products are the cyclic phosphate and *p*-nitrophenoxide as a result of a transesterification process involving the substrate hydroxyl functionality. The reactions were studied by using the pseudo-first-order method and results

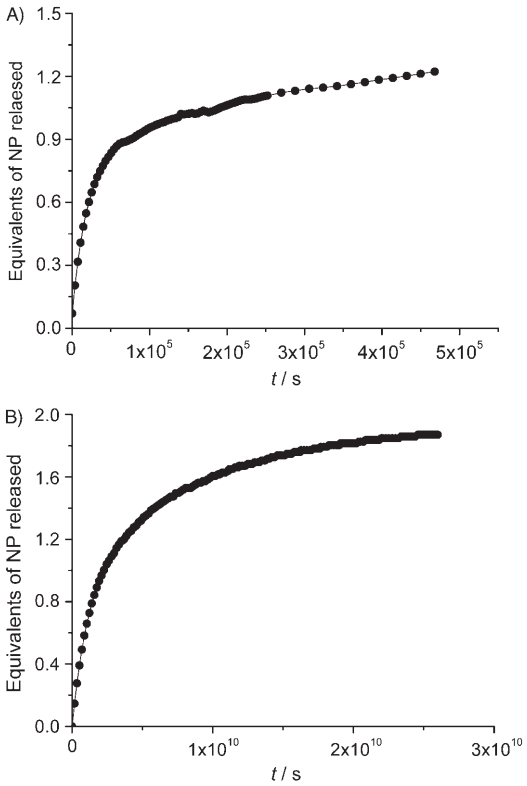

Figure 5. *p*-Nitrophenoxide (NP) release in the reaction of Zn^{II}–**4** with BNP at 25 °C and pH 9.0 ([buffer] = 5.0×10^{-2} M). Conditions: A) [Zn^{II}–**4**] = 5.0×10^{-4} M, [BNP] = 1.0×10^{-3} M; B) [Zn^{II}–**4**] = 1.0×10^{-3} M, [BNP] = 2.0×10^{-5} M.

showed that they were first-order in both the metal complex and in HPNP over the concentration range explored (Zn^{II} complexes 1×10^{-4}–1×10^{-3} M; BNP 5×10^{-4}–5×10^{-3} M). The pH dependence of the apparent second-order rate constants follow a bell-shaped profile in a similar manner to BNP (Figure 6). Fitting the curves by using the same model as before allowed the pK_a values of the active species to be determined (Table 3). In contrast with the experiment per-

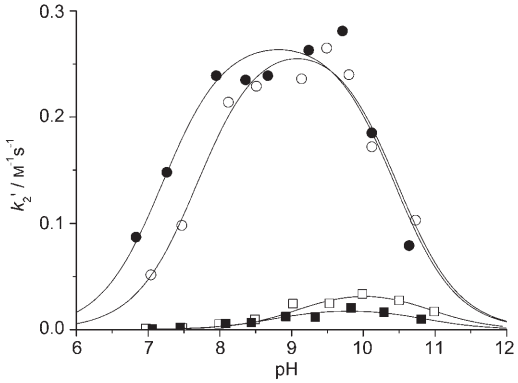

Figure 6. pH dependence of the apparent second-order rate constant (k_2') for the reaction between HPNP and Zn^{II} complexes of ligands **1** (□), **2** (■), **4** (●), and **5** (○) at 25 °C ([ligand] = [Zn^{II}] = 0.5–1.0×10^{-3} M, [HPNP] = 2×10^{-5} M, [buffer] = 5.0×10^{-2} M).

formed by using BNP as the substrate, the agreement between potentiometric and kinetic results is not as good. The kinetic pK_a values for the second deprotonation are similar, but the values obtained for the first deprotonation event are smaller. For complexes **4** and **5**, they are about 0.5 units lower than the results obtained by means of potentiometric titrations.[20] Inspection of the second-order rate constant values reported in Table 3 also reveals that the presence of the hydroxyl group in the ligand does not affect the reactivity of the system; in fact, the second-order rate constants for Zn^{II}–**1** and Zn^{II}–**2** are very similar, and those for Zn^{II}–**4** and Zn^{II}–**5** are identical. The acceleration at pH 7 is less impressive than in the case of BNP, but still remarkable. The pseudo-first-order rate constant for the cleavage of HPNP in the presence of Zn^{II}–**4**, at 1 mM concentration, is $(1.0\pm0.1)\times10^{-4}\ s^{-1}$ and this amounts to a rate enhancement of four orders of magnitude with respect to the background reaction ($k_\psi=(2.0\pm0.5)\times10^{-8}\ s^{-1}$, 25 °C, pH 7.0).

Discussion

A simple glance at the Brønsted plot reported in Figure 7 reveals the main results obtained in this study. The plot reports the reactivity data, from literature[21] and the present

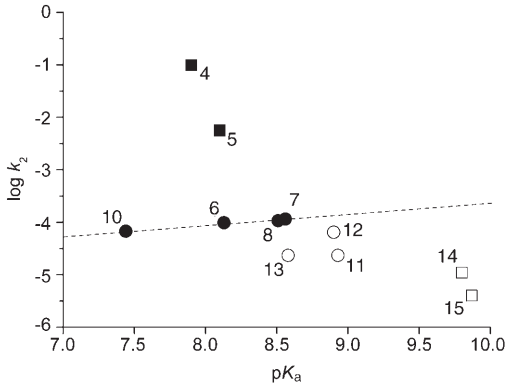

Figure 7. Brønsted plot (log k_2 vs. kinetic pK_a) for the BNP cleavage catalyzed by using Zn^{II} complexes in water at 25 °C. Ligands *cis,cis*-triaminocyclohexane (**6**), *all-cis*-2,4,6-triamino-1,3,5-trihydroxycyclohexane (**7**), *all-cis*-2,4,6-triamino-1,3,5-trimethoxycyclohexane (**8**), 1,5,9-triazacyclododecane (**10**), diethylentriamine(**11**), *N*-(2-aminoethyl)-1,3-propanediamine (**12**), dipropylentriamine (**13**), 1,4,8,11-tetrazacyclotetradecane (**14**), tris(2-aminoethyl)amine (**15**). The dashed line shows the linear fit of the reactivity data for the complexes of the cyclic ligands **6**–**10** (see ref. [21]).

work, for the cleavage of BNP, promoted by using several Zn^{II} complexes of tridentate and tetradentate polyamines with different structures, as a function of the pK_a values of the reactive species. Complexes Zn^{II}–**4** and Zn^{II}–**5** are far more reactive than any other mononuclear Zn^{II} complexes and such remarkable reactivity is due to the presence of different organic groups built into the ligand structure. However, the mechanism for the cleavage of phosphate esters promoted by using the Zn^{II} complexes of ligands **1**–**5** is rather complex and the sources of such reactivity enhancements probably arise from a delicate balance of several factors.

The commonly accepted reaction pathway for the cleavage of *p*-nitrophenyl phosphate esters by using metal complexes involves the following key steps: deprotonation of a metal-bound species to form the effective nucleophile, binding of the substrate to the metal complex, intracomplex nucleophilic attack on the substrate with the departure of the leaving group, and possibly regeneration of the catalyst.[1,3–4] The presence of the 6-aminopyridine and/or hydroxyl groups in the ligand structures may influence most of these stages.

The structures of the complexes should be taken into account first. Ligands **1**–**5** strongly bind Zn^{II} through the two pyridine and the tertiary amino nitrogen atoms. Potentiometric titrations also reveal that the metal coordination sphere contains at least two species that can be deprotonated. For the complexes of **1** and **5**, such species are clearly water molecules, whereas in the case of **2**, **3**, and **4**, coordination of the ligand hydroxyl group to the metal ion is possible (these complexes also contain a water molecule as the other metal-bound species for deprotonation). The NMR spectroscopic titration of Zn^{II}–**4** supports such a hypothesis because the resonances of the protons of the hydroxypropyl arm are affected by both of the deprotonation events occurring in the metal coordinating sphere, as one would expect if the hydroxyl group was coordinated to the Zn^{II} ion within the pH interval explored. Evidence of coordination of the hydroxyl group is provided by the formation of phosphorylated ligands in the reactions of Zn^{II}–**2** and Zn^{II}–**4** with BNP, which indicates that the hydroxyl group is the active nucleophile for substrate cleavage.

These indications were utilized to define the starting geometries in the DFT calculations for the structures of the mono-deprotonated Zn^{II}–**2** and Zn^{II}–**4** complexes. The optimized structures obtained give a reasonable insight into the spatial configuration of the complex. The donor atoms around the Zn^{II} ion are arranged in a distorted trigonal bipyramid geometry, and in Zn^{II}–**4**, the 6-amino groups are placed in the correct position to donate two hydrogen bonds to the apical metal-coordinated species. The two optimized structures obtained for the alkoxide species (Figures 3B and C) do not represent the ideal, in which the apical species that can be deprotonated coordinates to the metal and interacts with the whole network of hydrogen bonds provided by the two amino groups. This is probably a result of steric factors or the reluctance of a water molecule to accept two hydrogen bonds and be involved in metal coordination at the same time. The latter point may be the source of the unexpected decrease of the Zn^{II}-complex-formation constant observed with ligands **4** and **5** relative to **1** and **2** (Table 1).

On the other hand, the optimized structure of the hydroxide complex (Figure 3A) shows that the formation of intracomplex hydrogen bonds between the 6-amino groups and the apical metal-bound species is very efficient when the water molecule is deprotonated to form a hydroxyl anion.

This deprotonation should lead to an increase in the acidity of the apical water molecule in Zn^{II}–**4** relative to Zn^{II}–**2**, and in fact, the pK_a values of the metal-bound species, either the hydroxyl group or water molecules, decrease by 0.5–0.6 units on going from **2** to **4** and also from **1** to **5** (Table 1). However, the effect is rather small relative to the 1.5 units difference reported by Mareque-Rivas and co-workers for the Zn^{II} complex of bis[(6-amino-2-pyridylmethyl)-*N*-(2-pyridylmethyl)]amine, which is a comparable structure with the same number of intracomplex hydrogen bonds.[22] It is also surprising that the acidity increase observed involves both of the species that can be deprotonated, even if the one in the equatorial position (either the hydroxyl group in Zn^{II}–**4** or a water molecule in Zn^{II}–**5**) is not ideally positioned to interact with the pyridine amino groups.

These apparently puzzling results may be explained if one considers that the pK_a values measured by means of potentiometric titrations are macroscopic values that may be attributed to different microscopic species as indicated in Scheme 1. In the case of Zn^{II}–**4**, theoretical calculations

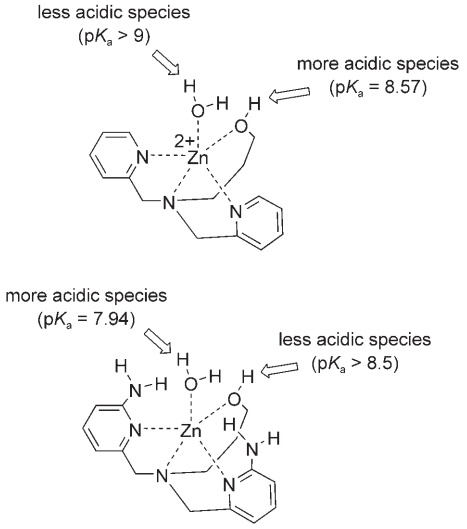

Scheme 1. Tentative identification of the microscopic pK_a values of the metal-bound species in Zn^{II}–**2** and Zn^{II}–**4**.

clearly point to the apical water molecule as the most acidic site in the complex; hence, the first potentiometric pK_a value measured can be attributed to this group. On the other hand, calculations indicate that the acidities of the two metal-bound species in Zn^{II}–**2** should be similar. However, it is likely that in this complex one of the two metal-bound species is somewhat more acidic (a difference of 0.5–1 logarithmic units between the two microscopic pK_a values is fully compatible with the results of the calculations). If we suppose that the more acidic species in complex Zn^{II}–**2** is the hydroxyl group, then we know that the species responsible for the first deprotonation is not the same for complexes Zn^{II}–**2** and Zn^{II}–**4**. As a consequence, the true effect of the intracomplex hydrogen bonds cannot be fully accounted for by the difference of 0.6 logarithmic units observed between the first macroscopic dissociation constants of the two complexes, but could be greater and probably closer to 1.5 as expected. At the same time, a change in the most acidic species, as a result of the presence of the intracomplex hydrogen bonds, would also influence the second macroscopic constant. In fact, the second deprotonation event in Zn^{II}–**4** would occur on the equatorial hydroxyl group, which is intrinsically more acidic than the apical water molecule that is the second species to dissociate in Zn^{II}–**2**. This hypothesis also explains why the presence of a single hydrogen bond in complex Zn^{II}–**3** does not result in any apparent decrease of the first pK_a value of the metal-bound species. The pK_a decrease of 0.46 logarithmic units, again reported by Mareque-Rivas and co-workers in the case of a single hydrogen bond,[22] could not be sufficient to produce a change in the most acidic species in the complex (a small decrease in the pK_a value relative to that in complex Zn^{II}–**2** is observed only for the second deprotonation constant). Of course, the same conclusions can also be drawn for complex Zn^{II}–**5**, in which a water molecule takes the place of the hydroxyl group coordinated to the equatorial free site.

The influence of the two deprotonation events on the reactivity of the systems is highlighted by the bell-shaped pH reactivity profiles shown in Figure 4. A similar behavior was observed in other phosphate cleavage reactions promoted by using metal-ion complexes and indicates that the deprotonation of the two acidic metal-bound species have opposite effects, the first one leading to a reactivity increase and the second one to a decrease.[3] According to the commonly proposed mechanism, the first deprotonation leads to the formation of the active nucleophile (a metal-bound hydroxide or alkoxide), whereas the second deprotonation forms a second anionic species that strongly binds to the metal so that the coordination sites available on the metal ion become saturated and this leaves little or no chance for coordination of the substrate.

Hence, the reactive species in such reactions is the mono-deprotonated complex. DFT calculations suggest that for the Zn^{II}–**4** complex, this mono-deprotonated species essentially exists in the reaction solution in the hydroxide form. On the contrary, the observed formation of the phosphorylated ligand in the reaction with BNP indicates that the alkoxide form is the one involved in substrate cleavage. In fact, both mono-deprotonated forms are likely to exist in equilibrium, although shifted toward the hydroxide complex, in which the reactive species is the one present in smaller amounts.[7b] The water molecule bound to the alkoxide complex is easily displaced by the anionic substrate that is better at accommodating the two hydrogen bonds from the neighboring pyridine 6-amino groups. Thus, coordination of the phosphate ester to the metal ion results in its activation towards nucleophilic attack, owing to the Lewis acidity of the Zn^{II} ion and to the effect of the two intracomplex hydrogen bonds. Comparison of the second-order rate constants in Table 3 indicates that activation of the substrate by means

of one or two hydrogen bonds produces a 9-fold and 230-fold reactivity increase, respectively. Of course, such values may be underestimated because the second-order rate constants are calculated over the whole complex concentration.

The alkoxide nucleophile in Zn^{II}–**4** leads to a 17-fold increase in reactivity with respect to the metal-bound hydroxide of Zn^{II}–**5**. Metal-bound alkoxides are better nucleophiles than metal-bound hydroxides in several cases and this effect was attributed to a weaker solvation of the oxygen atom by water owing to the steric hindrance of the lipophilic alkyl moiety.[7a]

The fate of the reaction after the attack of the nucleophile on the substrate depends upon the ligand structure and the experimental conditions employed (Scheme 2). BNP cleavage promoted by Zn^{II}–**5** occurs, as demonstrated by means of NMR spectroscopy experiments, through the hydrolysis of the substrate with formation of *p*-nitrophenoxide and *p*-nitrophenyl phosphate. In this case, a metal-bound water molecule is the active nucleophile and decomplexation of the product regenerates the catalyst for further reaction. However, the catalytic efficiency is decreased because the *p*-nitrophenyl phosphate (MNP) produced is more strongly bound by Zn^{II}–**5** than BNP, which results in product inhibition (see the Supporting Information).

For Zn^{II}–**4**, which is the most reactive complex, the cleavage reaction (see Scheme 2) is a transesterification process because the phosphorylated complex that results from the nucleophilic attack of the alkoxide species is not subsequently hydrolyzed to restore the reactive system. This result is somewhat surprising because the phosphorylated arm is still a *p*-nitrophenyl phosphate diester that could undergo an intramolecular attack by a metal-bound water molecule followed by release of the second *p*-nitrophenoxide molecule.[7a] Further reaction is probably prevented by two factors. First, it is likely that once the phosphorylated hydroxypropyl arm is formed it leaves the metal ion because its coordination requires the formation of an eight-membered ring. Second, even if such coordination could occur, the phosphate oxygen atom would probably occupy the equatorial position so that the only nucleophile available would be a modestly reactive, hydrogen-bonded apical hydroxide.

However, when the reaction occurs in the presence of an excess of BNP relative to the Zn^{II} complex, the fast formation of the phosphorylated complex is followed by a slow release of *p*-nitrophenoxide. NMR spectroscopy experiments indicate that this slower reaction is accompanied by the formation of MNP. Hydrolysis of the phosphorylated arm does not occur so formation of MNP can only result from BNP hydrolysis. This result indicates that once the phosphorylated hydroxypropyl arm is detached from the metal ion then a water molecule takes its place so that the resulting structure of the complex resembles Zn^{II}–**5** and it promotes the hydrolysis of BNP in the same way.

On the other hand, when the reaction is performed in the presence of an excess of Zn^{II}–**4**, two equivalents of *p*-nitrophenoxide are released for each molecule of BNP. In this case, the only possible source of the second equivalent of *p*-nitrophenoxide is from the cleavage of the phosphorylated hydroxypropyl arm. As such a reaction only occurs in the presence of an excess of complex, the most likely explanation is that the phosphorylated hydroxypropyl arm undergoes a nucleophilic attack by a second molecule of complex, which is accompanied by the release of the second molecule of *p*-nitrophenoxide and the formation of a dimer made by two Zn^{II}–**4** molecules linked by a phosphate bridge.[23]

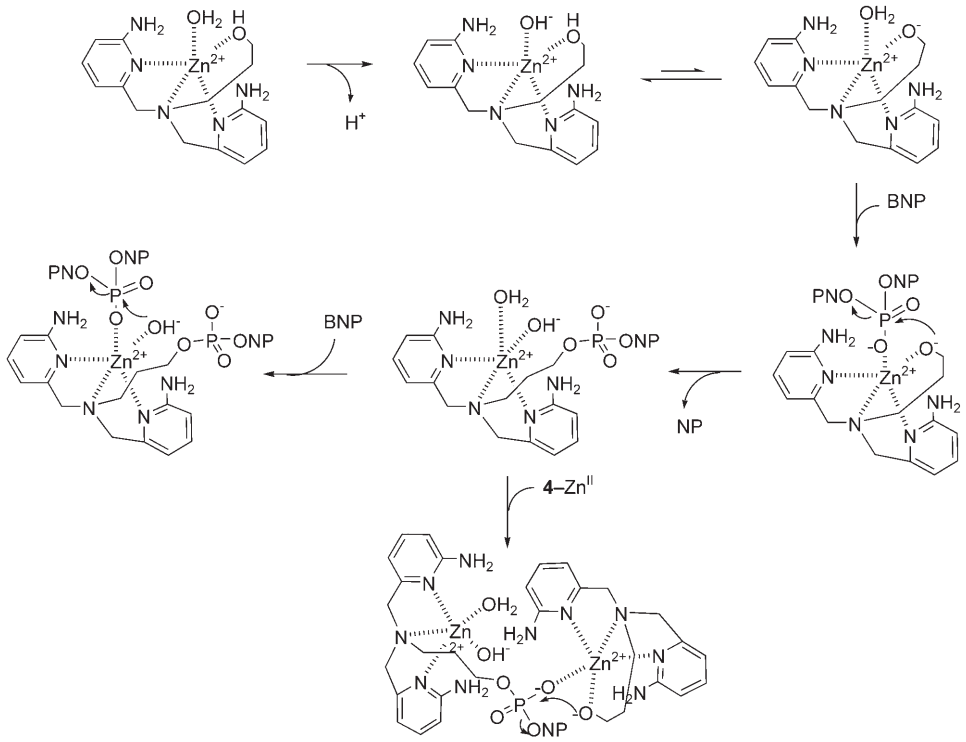

Scheme 2. Proposed mechanism for BNP cleavage by using Zn^{II}–**4** complexes.

The reactivity of the complexes toward HPNP shows some interesting peculiarities. First, complexes of ligands that do not contain a hydroxypropyl arm have the same reactivity as the corresponding ones with the hydroxyl group. This result, which is different from that from the reaction with BNP, is in agreement with the accepted mode of cleavage of HPNP, which implies that the substrate hydroxyl group is the effective nucleophile,[21,24] and as a consequence, there is little influence of other metal-bound nucleophiles on the reaction

rate. NMR spectroscopy experiments also show that the product of the reaction is, in each case, the cyclic phosphate diester resulting from substrate transesterification. The second peculiarity allows some considerations on the two generally proposed mechanisms for metal-complex-promoted HPNP transesterification. One pathway involves deprotonation of the substrate hydroxyl group by a metal-bound hydroxide (Scheme 3A), which acts as a general base catalyst. Another pathway (Scheme 3B) implies that there is

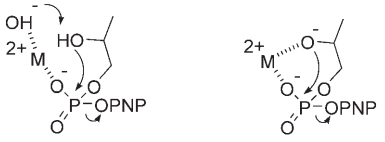

Scheme 3. Possible pathways for HPNP cleavage by using metal complexes.

direct coordination of the deprotonated substrate hydroxyl group to the metal ion and subsequent nucleophilic attack on the phosphorous center.

The two mechanisms are kinetically indistinguishable and evidence in favor of each has been reported.[24] Recently, no solvent kinetic isotopic effect was observed for the cleavage of either HPNP or related substrates by using Zn^{II} complexes. This finding was regarded as strong evidence in favor of the nucleophilic mechanism[21,25] (Scheme 3B) and rules out the possibility of concerted Brønsted general acid–base catalysis to couple the formation of the deprotonated alkoxide nucleophile with the protonation of the leaving group.[25] For the complexes reported here, it is interesting to note that the first kinetic pK_a values determined from fitting the pH reactivity profiles are notably different from those measured by means of potentiometric titrations. This observation could indicate that the metal-bound species that is deprotonated is different in each case. In the absence of substrate it is the metal-bound water molecule, and during the reaction it is the HPNP hydroxyl group that is deprotonated, as foreseen by the nucleophilic mechanism.

Aside from the mechanistic hypothesis, Figure 8 reveals that the activation effect of the two hydrogen-donating groups appears to be similar, albeit smaller, than the effect observed in the reaction with BNP. Table 3 reveals that Zn^{II}–**5** is only 13-fold more reactive than Zn^{II}–**2**. Previously, we have found that HPNP is less affected by the Lewis acid activation of the substrate than BNP[21] so that the smaller effect of the intracomplex hydrogen bonds on the cleavage rate is in full agreement with this observation.

Conclusion

The reactivity of the Zn^{II} complexes investigated in this study highlights the possibility of obtaining efficient phosphate ester cleavage systems by means of the cooperative action of metal ions and multiple organic groups. The overall result of the different acceleration effects—alkoxide nucleophile activation, double H-bond and Zn^{II} Lewis acid substrate activation—makes the Zn^{II}–**4** system capable of promoting BNP cleavage with remarkable activity. A reactivity increase of at least three orders of magnitude can be estimated on the basis of the effects of the single groups, which, combined with the benefits resulting from the low pK_a value of the active nucleophile, produces an acceleration of the BNP cleavage at pH 7 by six orders of magnitude. In particular, the implementation of the structure of the reactive complex with groups capable of forming intramolecular hydrogen bonds with the substrate emerges as the most important feature of the system. Work is in progress in our laboratory to obtain more efficient systems based on this strategy.

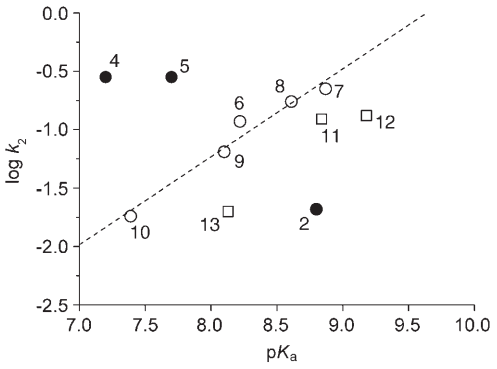

Figure 8. Brønsted plot (log k_2 vs. kinetic pK_a) for HPNP cleavage catalyzed by using Zn^{II} complexes in water at 25 °C. Ligands **2**, **4**–**8**, and **10**–**13** as in Figure 7 and 1,4,7-triazacyclononane (**9**). The dashed line shows the linear fit of the reactivity data for the complexes of cyclic ligands **6**–**10** (see ref. [21]).

Experimental Section

General: NMR spectra were recorded by using a Bruker AC250F spectrometer operating at 250 MHz for ^{1}H and 62.9 MHz for ^{13}C and a Bruker AV300 spectrometer operating at 300 MHz for ^{1}H and 121.5 MHz for ^{31}P. Potentiometric titrations were performed by using a Metrohom 716 DMS Titrino dynamic titrator. UV-visible spectra and kinetic traces were recorded on Perkin–Elmer Lambda 16 and Lambda 45 spectrophotometers equipped with thermostated multiple-cell holders.

$Zn(NO_3)_2$ was an analytical grade product. Metal-ion stock solutions were titrated against ethylene diamine tetraacetic acid (EDTA) by following standard procedures. The buffer components were used as supplied by the manufacturers: acetic acid (Aldrich), 2-morpholinoethanesulfonic acid (MES, Fluka), 4-(2-hydroxyethyl)-1-piperazineethanesulfonic acid (HEPES, Sigma), 4-(2-hydroxyethyl)-1-piperazinepropanesulfonic acid (EPPES, Sigma), 2-(*N*-cyclohexylamino)ethanesulfonic acid (CHES, Sigma), 3-(cyclohexylamino)-1-propanesulfonic acid (CAPS, Sigma). BNP from Aldrich was used as received, whereas HPNP was prepared and purified as a barium salt by following literature methods.[26]

Computational details: Geometry optimizations were first run at the B3LYP/6-31G(d,p) level of theory. The final geometries were then tested by using frequency calculations to check that they were an energy mini-

mum. The optimized structures were used as starting points for additional optimizations, and final energy calculations, at the B3LYP/6-311++G-(d,p) level, without a frequency check. Minor changes in the geometry were observed on moving from the low (small basis set) to the high (large basis set) level of theory. For complex **2**, only the first level of theory was employed. All calculations were run by using the software package Gaussian 03.[27] Self-consistent reaction field calculations were run by using the integral equation formalism version of the PCM.[28] Calculations have been run on an IBM SP5 instrument at the CINECA SuperComputing Center, Bologna, Italy.

Potentiometric titrations: Protonation constants and Zn^{II} complex-formation constants for ligands **1**–**5** were determined by means of pH potentiometric titrations (25 °C, 0.10 M NaCl). Solutions of the hydrochloride salts of the ligands (approximately 1×10^{-3} M), and when necessary $Zn(NO_3)_2$, were titrated by using a 0.1 M sodium hydroxide solution. The electrode system was calibrated by titrating a 0.01 M solution of HCl to obtain a pK_w value of 13.78. The data for pH versus volume of NaOH added were fitted by using the computer program BEST[29] to obtain the desired protonation and complex-formation constants.

NMR spectroscopic titration: Complex $[Zn^{II}(\mathbf{4})(ClO_4)_2]$ (see the Supporting Information) was dissolved in D_2O (0.8 mM) and the pD was adjusted to the desired value by adding concentrated NaOD and DCl solutions (the correction pD = pH+0.4 was applied to the pH meter reading of the buffers).[30] The ^{1}H NMR spectrum was then recorded. Chemical shift versus pD data were fitted according to Equation (1):

$$\delta_{oss}=\frac{\delta(H_2A)}{(1+K_a^1/[H^+]+K_a^2K_a^1/[H^+]^2)}+\frac{\delta(HA)}{(K_a^1/[H^+]+1+[H^+]/K_a^2)}+\frac{\delta(A)}{(1+[H^+]/K_a^2+[H^+]^2/K_a^2K_a^1)} \quad (1)$$

The obtained values were $pK_a^1=8.2\pm0.2$, $pK_a^2=10.0\pm0.2$.

Kinetic measurements: The kinetic traces were recorded on Perkin–Elmer Lambda 16 and Lambda 45 spectrophotometers equipped with thermostated multiple cell holders. The reaction temperature was maintained at 25 ± 0.1 °C. Metal complexes of ligands **1**–**5** were formed in situ by mixing equimolar amounts of metal ion and ligand in the appropriate buffer. The reactions were started by adding a 2.0×10^{-2} (initial rate method) or 2.0×10^{-3} M (pseudo-first-order method) solution of substrate (20 μL) to a solution of complex (2 mL) and was monitored by following the absorption of *p*-nitrophenoxide at $\lambda=400$ nm.

When the initial-rate method was used, reactions were followed until about 5% of the substrate had been cleaved. The pseudo-first-order rate constants (k_ψ) were obtained from the slope of the absorbance versus time data (the fit error was always less than 5%) divided by the molar absorbtivity of the *p*-nitrophenoxide and the concentration of substrate. When the pseudo-first-order method was used, reactions were followed up to at least 90% substrate cleavage and the pseudo-first-order rate constants (k_ψ) were obtained by using nonlinear regression analysis of the absorbance versus time data according to Equation (2):

$$A=A_{inf}(1-e^{-k_\psi t}) \quad (2)$$

The fit error for the rate constant was always less than 5%.

Apparent pH-dependent second-order rate constants (k'_2) were obtained by means of linear-regression fitting of the k_ψ versus metal-complex concentration data. Kinetic K^n_a values and second-order rate constants (k_2) for the mono-deprotonated complexes were obtained by using nonlinear regression analysis of the apparent second-order rate constants versus pH data according to Equation (3):

$$k'_2=\frac{k_2}{([H^+]/K_a^1+1+K_a^2/[H^+])} \quad (3)$$

[1] N. H. Williams, B. Takasaki, M. Wall, J. Chin, *Acc. Chem. Res.* **1999**, *32*, 485–493. Different half-life values for the hydrolysis of DNA and RNA have been reported in the literature and are discussed herein.

[2] a) J. Weston, *Chem. Rev.* **2005**, *105*, 2151–2174; b) M. J. Jedrzejas, P. Setlow, *Chem. Rev.* **2001**, *101*, 608–618; c) J. A. Cowan, *Chem. Rev.* **1998**, *98*, 1067–1087; d) D. E. Wilcox, *Chem. Rev.* **1996**, *96*, 2435–2458; e) N. Sträter, W. N. Lipscomb, T. Klabunde, B. Krebs, *Angew. Chem.* **1996**, *108*, 2158–2191; *Angew. Chem. Int. Ed. Engl.* **1996**, *35*, 2024–2055.

[3] J. Chin, *Acc. Chem. Res.* **1991**, *24*, 145–152.

[4] a) F. Mancin, P. Scrimin, P. Tecilla, U. Tonellato, *Chem. Commun.* **2005**, 2540–2548; b) A. K. Yatsimirsky, *Coord. Chem. Rev.* **2005**, *249*, 1997–2011; c) J. R. Morrow, O. Iranzo, *Curr. Opin. Chem. Biol.* **2004**, *8*, 192–200; d) G. Parkin, *Chem. Rev.* **2004**, *104*, 699–768; e) S. J. Franklin, *Curr. Opin. Chem. Biol.* **2001**, *5*, 201–208; f) R. Ott, R. Krämer, *Appl. Microbiol. Biotechnol.* **1999**, *52*, 761–767; g) E. L. Hegg, J. N. Burstyn, *Coord. Chem. Rev.* **1998**, *173*, 133–165.

[5] R. Krämer, *Coord. Chem. Rev.* **1999**, *182*, 243–261.

[6] R. Breslow, D. Berger, D. Huang, *J. Am. Chem. Soc.* **1990**, *112*, 3686–3687.

[7] a) E. Kimura, Y. Kodama, T. Koike, M. Shiro, *J. Am. Chem. Soc.* **1995**, *117*, 8304–8311; b) M. J. Young, D. Wahnon, R. C. Hynes, J. Chin, *J. Am. Chem. Soc.* **1995**, *117*, 9441–9447.

[8] E. Kövári, R. Krämer, *J. Am. Chem. Soc.* **1996**, *118*, 12704–12709.

[9] H. Aït-Haddou, J. Sumaoka, S. L. Wiskur, J. F. Folmer-Andersen, E. V. Anslyn, *Angew. Chem.* **2002**, *114*, 4185–4188; *Angew. Chem. Int. Ed.* **2002**, *41*, 4013–4016.

[10] The same system produces a rate acceleration for the hydrolysis of a cyclic phosphate diester (2′,3′-cAMP) of four orders of magnitude: M. Wall, B. Linkletter, D. Williams, A. M. Lebuis, R. C. Hynes, J. Chin, *J. Am. Chem. Soc.* **1999**, *121*, 4710–4711.

[11] G. Feng, J. C. Mareque-Rivas, R. T. M. de Rosales, N. H. Williams, *J. Am. Chem. Soc.* **2005**, *127*, 13470–13471.

[12] The same authors obtained an increase in the rate of HPNP transesterification by two orders of magnitude by using the Zn^{II} complex of bis(6-amino-2-pyridinylmethyl)-2-ethanolamine, which features two hydrogen-bond-donating groups: G. Feng, J. C. Mareque-Rivas, N. H. Williams, *Chem. Commun.* **2006**, 1845–1847.

[13] M. Livieri, F. Mancin, U. Tonellato, J. Chin, *Chem. Commun.* **2004**, 2862–2863.

[14] J. K. Romary, J. D. Barger, J. E. Bunds, *Inorg. Chem.* **1968**, *7*, 1142–1145.

[15] a) M. Brauer, L. Perez-Lustres, J. Weston, E. Anders, *Inorg. Chem.* **2002**, *41*, 1454–1463; b) J. Xia, Y. Shi, Y. Zhang, Q. Miao, W. Tang, *Inorg. Chem.* **2003**, *42*, 70–77.

[16] Binding energies for this additional water molecule have been calculated (in the gas phase) and were found to be about 17 kcal mol^{-1} in the case of the hydroxide form and 13 kcal mol^{-1} in the case of the alkoxide one (Figure 3C); such values support the assumption of explicitly including an additional solvent molecule.

[17] Lower-level calculations (B3LYP/6-31G*) indicate that similar structures represent energy minima also in the case of the non-deprotonated complex.

[18] J. Chin, M. Banaszczyk, V. Jubian, X. Zou, *J. Am. Chem. Soc.* **1989**, *111*, 186–190.

[19] The diester *p*-nitrophenyl ethyl phosphate was investigated as a model compound; the ^{31}P NMR spectrum shows a single signal (triplet) at $\delta=-9.45$ ppm.

[20] Very similar results were obtained for the HPNP transesterification by using the closely related Zn^{II} complex of bis(6-amino-2-pyridinylmethyl)-2-ethanolamine: see ref. [12].

[21] L. Bonfá, M. Gatos, F. Mancin, P. Tecilla, U. Tonellato, *Inorg. Chem.* **2003**, *42*, 3943–3949.

[22] J. C. Mareque-Rivas, R. Prabaharan, R. T. M. de Rosales, *Chem. Commun.* **2004**, 76–77.

[23] Under these conditions, the dependence of the rate from the complex concentration is second-order.

[24] a) I. O. Fritsky, R. Ott, H. Pritzkow, R. Krämer, *Chem. Eur. J.* **2001**, *7*, 1221–1231; b) S. Mikkola, E. Stenman, K. Nurmi, E. Yousefi-Salakdeh, R. Strömberg, H. Lönnberg, *J. Chem. Soc. Perkin Trans. 2* **1999**, 1619–1625; c) P. Molenveld, J. F. J. Engbersen, H. Kooijman, A. L. Spek, D. N. Reinhoudt *J. Am. Chem. Soc.* **1998**, *120*, 6726–6737; d) S. Liu, A. D. Hamilton, *Tetrahedron Lett.* **1997**, *38*, 1107–1110; e) M. Kalesse, A. Loos, *Liebigs Ann.* **1996**, 935–939.
[25] M.-Y. Yang, O. Iranzo, J. P. Richard, J. R. Morrow, *J. Am. Chem. Soc.* **2005**, *127*, 1064–1065.
[26] D. A. Brown, D. A. Usher, *J. Chem. Soc.* **1965**, 6558–6564.
[27] Gaussian 03, Revision B.05, M. J. Frisch, G. W. Trucks, H. B. Schlegel, G. E. Scuseria, M. A. Robb, J. R. Cheeseman, J. A. Montgomery, Jr., T. Vreven, K. N. Kudin, J. C. Burant, J. M. Millam, S. S. Iyengar, J. Tomasi, V. Barone, B. Mennucci, M. Cossi, G. Scalmani, N. Rega, G. A. Petersson, H. Nakatsuji, M. Hada, M. Ehara, K. Toyota, R. Fukuda, J. Hasegawa, M. Ishida, T. Nakajima, Y. Honda, O. Kitao, H. Nakai, M. Klene, X. Li, J. E. Knox, H. P. Hratchian, J. B. Cross, V. Bakken, C. Adamo, J. Jaramillo, R. Gomperts, R. E. Stratmann, O. Yazyev, A. J. Austin, R. Cammi, C. Pomelli, J. W. Ochterski, P. Y. Ayala, K. Morokuma, G. A. Voth, P. Salvador, J. J. Dannenberg, V. G. Zakrzewski, S. Dapprich, A. D. Daniels, M. C. Strain, O. Farkas, D. K. Malick, A. D. Rabuck, K. Raghavachari, J. B. Foresman, J. V. Ortiz, Q. Cui, A. G. Baboul, S. Clifford, J. Cioslowski, B. B. Stefanov, G. Liu, A. Liashenko, P. Piskorz, I. Komaromi, R. L. Martin, D. J. Fox, T. Keith, M. A. Al-Laham, C. Y. Peng, A. Nanayakkara, M. Challacombe, P. M. W. Gill, B. Johnson, W. Chen, M. W. Wong, C. Gonzalez, J. A. Pople, Gaussian, Inc., Wallingford CT, **2004**.
[28] a) M. Cossi, V. Barone, B. Mennucci, J. Tomasi, *Chem. Phys. Lett.* **1998**, *286*, 253–260; b) M. T. Cancès, B. Mennucci, J. Tomasi, *J. Chem. Phys.* **1997**, *107*, 3032–3041; c) B. Mennucci, J. Tomasi, *J. Chem. Phys.* **1997**, *106*, 5151–5158.
[29] A. E. Martell, R. J. Motekaitis, *Determination and Use of Stability Constants*, 2nd ed., VCH, New York, **1992**.
[30] R. G. Bates, *Solute-Solvent Interactions* (Eds.: I. F. Coetzer, C. D. Ritchie), Marcel Dekker, New York, **1969**.

Received: May 15, 2006
Revised: October 6, 2006
Published online: December 13, 2006

